Journal of Solid State Chemistry 182 (2009) 259–264

Contents lists available at ScienceDirect

Journal of Solid State Chemistry

journal homepage: www.elsevier.com/locate/jssc

Solvothermal crystal growth of $CuSbQ_2$ (Q = S, Se) and the correlation between macroscopic morphology and microscopic structure

Jian Zhou [a,c], Guo-Qing Bian [a], Qin-Yu Zhu [a,b], Yong Zhang [a], Chun-Ying Li [a], Jie Dai [a,b,*]

[a] Department of Chemistry and the Key Laboratory of Organic Synthesis of Jiangsu Province, Suzhou University, Suzhou 215123, PR China
[b] State Key Laboratory of Coordination Chemistry, Nanjing University, Nanjing 210093, PR China
[c] Department of Chemistry and Biology, Yulin Normal University, Yulin 537000, PR China

ARTICLE INFO

Article history:
Received 20 August 2008
Received in revised form
12 October 2008
Accepted 20 October 2008
Available online 5 November 2008

Keywords:
Solvothermal synthesis
Chalcogenidoantimonate
Crystal structure
Crystal growth

ABSTRACT

A low temperature solvothermal method has been successfully used for preparation of two semiconductor compounds $CuSbQ_2$ (Q = S(**1**), Se(**2**)) by the reactions of Cu, Sb and S(or Se) powders in 1,2-diaminopropane at 160 °C for 10 days. The crystal structure of **2** was determined first time using single crystal X-ray diffraction analyses. The structures of **1** and **2** are discussed in the view of covalent bonds and weak interactions. Double $CuSbQ_2$ layers are assembled to a 3-D network structure by Cu···Sb and Q···Sb secondary bonds. In contrast with the isostructure of the two materials, the crystal morphology of them is quite different, brick-like crystals for $CuSbS_2$ and plank-like crystals for $CuSbSe_2$. The phenomenon is related to their different inter-planar interactions. Semiconductor properties of the microcrystal samples are measured and the band gaps of **1** and **2** are 1.38 and 1.05 eV, respectively.

1. Introduction

Ternary copper-based chalcogenidoantimonates $CuSbQ_2$ (Q = S, Se) are important semiconductors with narrow band gap, which have many potential applications in infrared detectors, photovoltaic devices and solar cells [1]. Being promising materials, both the chalcogenidoantimonates have been studied by many working groups and prepared in a variety of ways for different purposes. Traditionally, these compounds were prepared by solid-state synthetic techniques, which required high temperature, high pressure, inert atmosphere protection [2]. Recently, milder and softer chemical approaches to these compounds (such as hydrothermal and solvothermal methods) have been paid great attention, because these methods are favorable for preparation of the materials with nanosize. For instance, Xie and coworkers prepared $CuSbS_2$ spherical nanoparticles with CuI, $SbCl_3$ and elemental S in ethylenediamine solution under solvothermal condition [3]. The high quality $CuSbS_2$ nanorods have been prepared by low temperature surfactant-assisted hydrothermal synthesis [4]. The $CuSbS_2$ thin film has also been obtained from aqueous solutions by Spray-Pyrolysis-Deposition [5]. Although some of these reports concern crystalline $CuSbS_2$, the crystal size is usually on nanoscale. To our knowledge, crystals in millimeter scale have not been grown *via* milder and softer chemical methods. In addition, $CuSbSe_2$ material, even in nanocrystalline form, has not been prepared by the low temperature route to date.

Crystal structure of $CuSbS_2$, which was obtained from a Rhar-el-Anz mineral sample (containing Cl and Fe traces) or prepared *via* solid-state reaction of Cu, Sb and S at 310 °C, was twice determined by X-ray powder diffraction [6]. It crystallized in orthorhombic space group Pnma with the slightly different lattice parameters, but complete descriptions of the crystal structure were not given. Single crystal of $CuSbS_2$ prepared *via* a flux method was determined latterly (2005) by Kyono using a four-circle diffractometer [7]. Their work mainly addresses the anisotropic bonds of the Sb coordination and stereochemical activity of the Sb $5s^2$ lone-pair electrons. The structure of $CuSbSe_2$ was originally determined only once (1964) by X-ray powder diffraction [8], but the conventional R factor of 0.2 is very high. The powder diffraction often suffers from the inevitable loss of information resulting from the collapse of 3D crystallographic data on to a 1D diffraction pattern. The variety in the stereochemistry of the transition metal chalcogenide could result in subtle structural modifications, so the best way to reveals the fine details of structure are single-crystal structure determination rather than the powder diffraction techniques [9].

In this work, we report a facile one-pot solvothermal method for growth of ternary $CuSbQ_2$ (Q = S, Se) crystals. Single crystals of $CuSbQ_2$ with approximative millimeter scale were successfully obtained by reaction of Cu, Sb and S (or Se) powders in 1,2-diaminopropane. Mainly because the ternary $CuSbQ_2$ are important materials, the structural data of the solvothermal prepared

* Corresponding author at: Department of Chemistry and the Key Laboratory of Organic Synthesis of Jiangsu Province, Suzhou University, Suzhou 215123, PR China. Fax: +86 512 658 80089.
E-mail address: daijie@suda.edu.cn (J. Dai).

0022-4596/$ - see front matter © 2008 Elsevier Inc. All rights reserved.
doi:10.1016/j.jssc.2008.10.025

$CuSbQ_2$ ($Q = S$(**1**), Se(**2**)) were redetermined by single crystal X-ray diffraction analyses with higher accuracy. More remarkably, the two isostructural compounds display different morphologies in crystals and the phenomena are discussed in the view of the correlation between crystal morphology (macroscopical) and crystal structure (microscopic). The electronic spectra and behaviors in semi-conductivity of compounds **1** and **2** are also presented.

2. Experimental

2.1. Synthesis

$CuSbS_2$(**1**): Single crystals of the compound suitable for X-ray crystallographic analysis were obtained by solvothermal reaction. The reagents of Cu (12.7 mg, 0.2 mmol), Sb (24.4 mg, 0.2 mmol), S (16 mg, 0.5 mmol), H_2O (0.2 mL) and dap (1 mL, 1,2-diaminopropane) were mixed in a thick Pyrex tube (ca. 20 cm long). The sealed tube was heated at 160 °C for 10 days to yield black crystals. The crystals were washed with ethanol and diethyl ether, dried and stored under vacuum (93% yield based on Cu). IR (cm^{-1}): 1628(s), 1458(w), 1389(w), 1289(w), 1250(m), 1196(m), 1057(m), 972(w), 887(w), 586(s).

$CuSbSe_2$ (**2**): The black crystals of **2** were prepared by a similar method as used in the synthesis of the crystals of **1** except that S powder was replaced by Se powder (yield 95%, based on Cu). IR (cm^{-1}): 1628(s), 1458(w), 1389(w), 1250(m), 1196(m), 1057(m), 964(w), 895(w), 594(s), 432(w).

2.2. Physical measurements

The morphologies of the samples were observed with a JSM-5600LV scanning electron microscope (SEM). FT-IR spectra were recorded with a Nicolet Magna-IR 550 spectrometer in dry KBr disks in the 4000–400 cm^{-1} range. Solid-state UV–vis-NIR spectra were measured with a Shimadzu UV-3150 spectrometer at room temperature in the range 200–2800 nm. The absorption data were calculated from the reflectance [10]. Powder XRD patterns were collected on a D/MAX-3C diffractometer using graphite-monochromatized Cu$K\alpha$ radiation ($\lambda = 1.5406$ Å). The conductivity measurements were made with a two-probe conductivity apparatus designed for pressed samples. Two cylindrical electrodes press onto the sample from opposite sides under a hydrostatic pressure of 1.67×10^7 Pa.

2.3. Crystal structure determination

Data collections were performed on a Rigaku Mercury CCD diffractometer using a ω-scan method with graphite monochromated Mo$K\alpha$ radiation ($\lambda = 0.071073$ nm) at 173(2) or 213(2) K to a maximum 2θ value. An absorption correction was applied for both compounds using a multi-scan correction method. The structures were solved by direct methods and refined by the full-matrix least squares on F^2 using SHELXL-97 software [11,12]. All atoms were refined anisotropically. Relevant crystal and collection data parameters and refinement results can be found in Table 1. Selected bond lengths, angles and important secondary interactions for compounds **1** and **2** are listed in SI-Tables 1 and 2, respectively.

Table 1
Crystal data and summary of X-ray data collection.

Chemical formula	$CuSbS_2$	$CuSbSe_2$
Formula weight (g/mol)	249.41	343.21
Crystal system	Orthorhombic	Orthorhombic
Space group	Pnma	Pnma
a (Å)	6.014(2)	6.299(2)
b (Å)	3.7882(12)	3.9734(12)
c (Å)	14.472(5)	15.005(5)
V (Å^3)	329.69(19)	375.5(2)
Z	4	4
Dcalc. (g cm^{-3})	5.025	6.071
Radiation (Å)	Mo$K\alpha$, 0.71073	Mo$K\alpha$, 0.71073
Temperature (K)	173(2)	213(2)
Crystal size (mm)	$0.50 \times 0.20 \times 0.20$	$0.30 \times 0.25 \times 0.06$
μ (mm^{-1})	15.607	31.977
2θ (max) (deg)	50.66	50.62
F(000)	448	592
Reflections collected	2994	3350
Unique reflections	353	393
Observations [$I > 2\sigma(I)$]	332	357
Parameters	26	27
$R1$ [$I > 2\sigma(I)$]	0.0290	0.0462
w$R2$ (all data)	0.0813	0.1141
Goodness of fit	1.036	1.027

3. Results and discussion

3.1. Synthesis of the compounds

The title compounds were obtained from a Cu/Sb/S(or Se)/dap mixture in a molar ratio of Cu/Sb/S(or Se) = 1:1:2.5 under identical solvothermal conditions. The morphology of the crystals of $CuSbS_2$ and $CuSbSe_2$ was measured by SEM and is illustrated in Fig. 1. The $CuSbS_2$ shows a large quantity of brick-like crystals (pillared crystals) with average scale of 10–20 μm (Fig. 1a). These blocks display many crystal faces, which result from different growth speed of the corresponding crystal planes. The crystals of $CuSbSe_2$ were in plank-like form with an average scale of 10–20 μm (Fig. 1b). Single crystals of $CuSbQ_2$ material with larger crystal size (mm scale) have also been obtained by prolonging the reaction time. Fig. 2 illustrates the single crystals of $CuSbSe_2$ material with larger size and displays different shapes, such as irregular hexagon (Fig. 2a), truncated quadrate (Fig. 2b) and truncated lozenge (Fig. 2c). The thickness of crystals of **2** (plank) is invariably very thin in comparing with that of **1** (brick), which is the obvious difference in morphology of the two crystals, although they are isostructural. This difference in crystal shape implies that some different entities of the microstructures should be related to, but what are they?

There are many reports on the formation of ternary copper-based chalcogenidoantimonates in organic amine solution under the solvothermal conditions. The organic amines act as structure directing agents or template agents, which usually incorporate into the final products, as exemplified by $[C_4H_{12}N_2]_{0.5}[CuSb_6S_{10}]$ ($C_4H_{12}N_2$ = piperazine) [13], $(amineH_2)_{0.5}Cu_2SbS_3$ (amine = ethylenediamine (en) [14], 1,3-diaminopropane [14], 1,4-diaminobutane [14], 1,6-diaminohexane [15], diethylenetriamine (dien) [15]), $[en]_{0.5}[Cu_2SbS_3]$ [16], $(dienH)Cu_3Sb_2S_5$ [15], $(tetaH_2)_{0.5}Cu_3Sb_2S_5$ (teta = triethylenetetramine) [15], $Cu_2SbSe_3 \cdot x$en (en = ethylenediamine, $x = 0.5$, 1) [17]. However, in the present compounds **1** and **2**, 1,2-diaminopropanes did not appear in the final products based on the results of single crystal structure determination and powder XRD analysis. The purity of the product has been checked by comparing its experimental and simulated XRD patterns. The diffraction peaks on both patterns corresponded well in position (SI-Figs. 1 and 2), proving the absence of the organic component in the crystals. The only similar

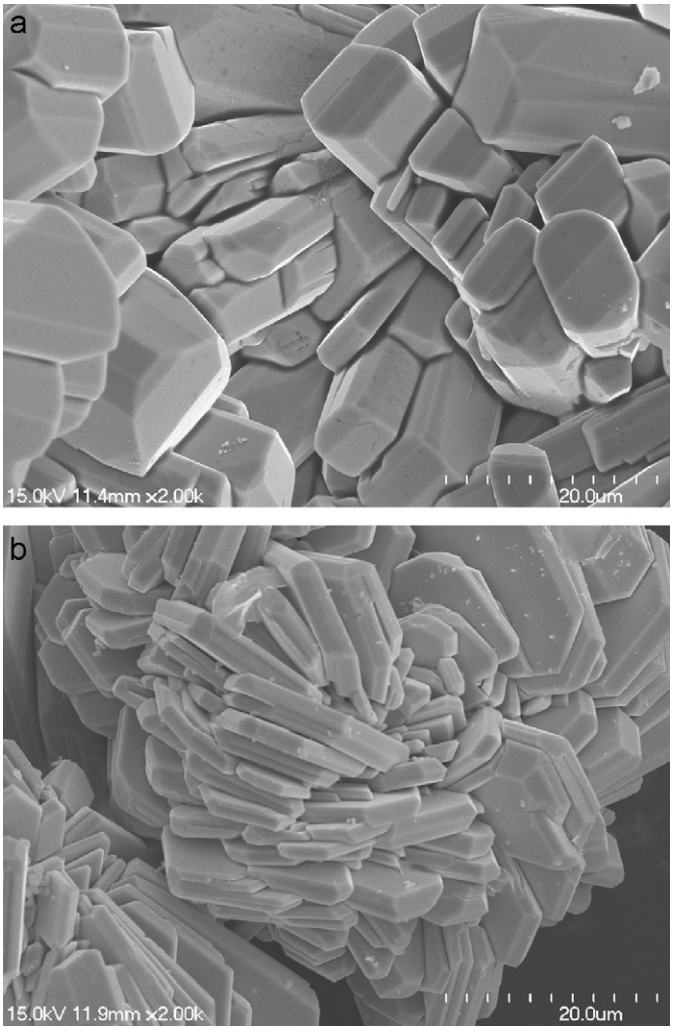

Fig. 1. SEM images of the as-synthesized $CuSbS_2$ (a) and $CuSbSe_2$ (b) (8days).

example was found by Qian and Xie group [3]. Spherical $CuSbS_2$ particles were prepared in en solution under the solvothermal conditions, but no single crystal was obtained in this way. In the view of material science, the pure inorganic phase will be more stable in suffering higher temperature and more stable in physical properties, and the lower temperature synthetic method for large size crystals of pure inorganic ternary chalcogenidomatelates is very important.

Although 1,2-diaminopropane(dap) is not incorporated into the final structures of both compounds, it plays multiple roles in the formation of pure $CuSbQ_2$ in this system. Besides acting as a solvent, it at least performs some other important roles. The first is that dap reacting with chalcogen powders offers Q^{2-} or Q_x^{2-} source [18]. A dark brown color is developed immediately when the sulfur reacts with dap, which indicates the formation of S^{2-} or S_x^{2-} anions, though the mechanism has not been proved yet. The second is that dap is a classical N-chelating ligand for transition metals; the formation of complex $[Cu(dap)_x]^+$, a intermediate generated on the surface of the metal, may promote the reaction of M with S or S_x^{2-} anion and control the speed of the crystal growth.

3.2. Description of the structure

Crystal data of $CuSbS_2$ (**1**) deposited with the ICSD database were only obtained by X-ray powder diffraction technique. Single crystal data of **1** was first deposited to the database of Fiz-Karlsruhe in this work, although the structure had been determined *via* a four-circle single crystal diffractometer recently by Kyono et al. [7]. Since the main structural characters of **1** had been described previously, it will not be discussed here again, except for those needed in comparing with the $CuSbSe_2$ (**2**). Compound **2**, $CuSbSe_2$, crystallizes in orthorhombic space group Pnma (No. 62) with four formula units in a unit cell. It is composed of 2-D double-layered structures with six-membered heterorings of Sb_2CuSe_3 and $SbCu_2Se_3$. These heterorings are self-condensed to form a honeycomb-like net (a single layer) extending in the (001) plane. Two single layers are connected

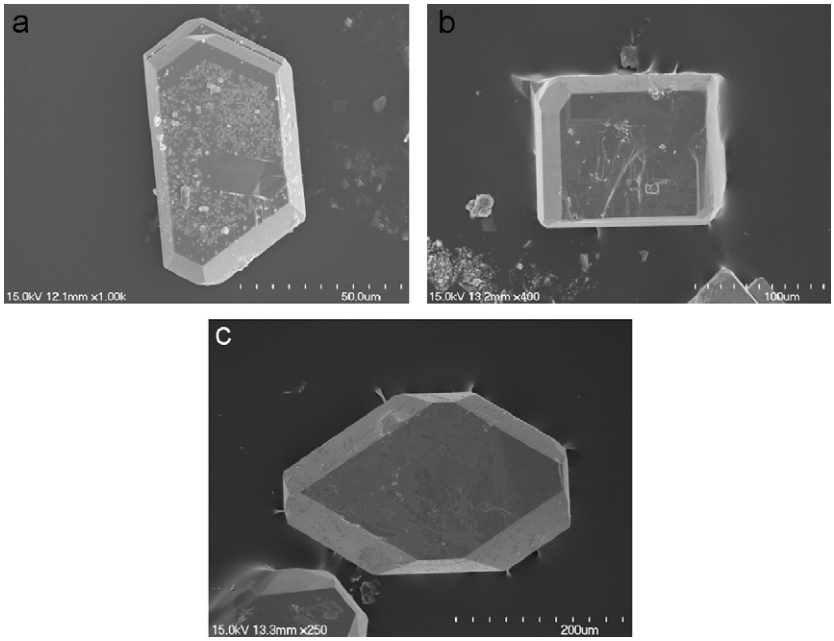

Fig. 2. SEM images of representative single crystals of $CuSbSe_2$.

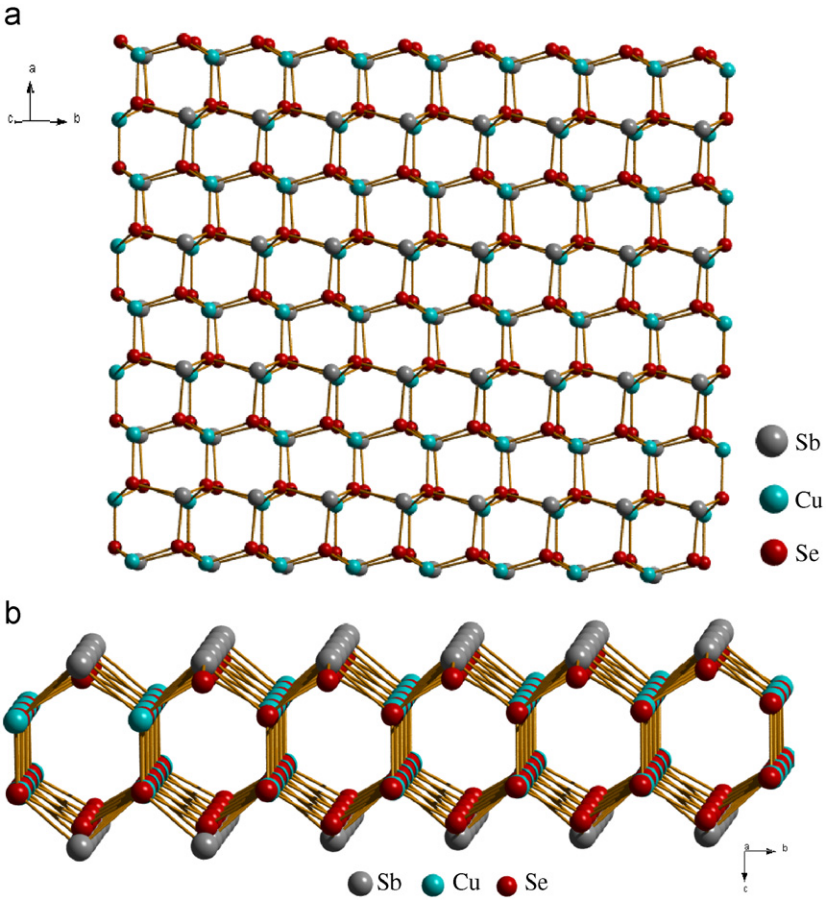

Fig. 3. (a) The 2-D double layer of **2** and (b) view down the *a*-axis of **2** showing 1-D channels.

via Cu–Se bonds forming a double-layered arrangement (Fig. 3a). When viewed down the *a*-axis, Cu and Sb atoms are hexagon-like arranged and connected to each other by Se atoms to form 1-D tunnel features (Fig. 3b). Compounds **1** and **2** are isostructural and details of crystal data in CIF format can be found in the Supporting Information. The similar double honeycomb-like sheets produced by fused six-membered heterorings are observed in $(enH)_2[Ag_5Sb_3S_8]$ [19], $(tetaH_2)[Ag_5Sb_3S_8]$ [20], and $(tetaH_2)_{0.5}Cu_3Sb_2S_5$ [15], those are anionic sheets.

It is interesting that there are significant secondary Sb⋯Cu interactions (3.417(2) Å for **1** and 3.473(2) Å for **2**) and Sb⋯Q interactions (3.107(2) Å for Sb⋯S and 3.198(1) Å for Sb⋯Se) between the layers, those distances are less than the sum of the respective van der Waals radii (3.60 Å for Sb⋯Cu, 3.80 Å for Sb⋯S and 4.20 Å for Sb⋯Se) [21]. The neighboring $CuSbQ_2$ layers are interconnected by these secondary interactions, resulting in a 3-D network structure (Fig. 4). In other similar layered compounds [14–17], organic components are generally sandwiched between the anionic layers *via* N–H⋯Q H-bonds, while the 3-D extended networks of **1** and **2** are constructed directly by weak secondary interlayer interactions.

In compounds **1** and **2**, the Sb atom is coordinated to three chalcogen atoms to form a SbQ_3 trigonal pyramidal geometry with typical bond lengths in the range 2.425(2)–2.5593(15) Å for **1** and 2.5707(18)–2.6994(13) Å for **2** [22]. The Cu atom has a distorted tetrahedral coordination with four *Q* atoms. The Cu–*Q* bond lengths are 2.306(2)–2.3253(14) Å for Cu–S and 2.404(2)–2.432(2) Å for Cu–Se. In addition, the Sb^{3+} ion, with the electronic configuration $4d^{10}5s^2$, is the heavy *p*-block metal, which possesses variable coordination behaviors caused by the stereo-chemically active lone pair. The sums of the *Q*–Sb–*Q* bond angles for both structures are 287.52(7)° for S and 285.72(6)° for Se, which point to a higher *p*-character of the Sb–*Q* bonds. Therefore, the $5s^2$ electron pair of Sb^{3+} ion in compounds **1** and **2** is mainly located on the lone pair in one direction of the tetrahedron, integrating with the SbQ_3 trigonal pyramid (Fig. 5a). The $SbCuQ_4$ polyhedron, considering with the Sb contact, can be described as a distorted mono-capped tetrahedron (Fig. 5b). The orientation of $5s^2$ lone pair always points towards the Cu center, resulting the additional relatively long Sb⋯Cu contact with adjacent $SbCuQ_2$ layer mentioned above. Therefore the lone pair of Sb^{3+} ion plays a very important role in the interlayer interaction. The sums of the *Q*–Sb–*Q* bond angles also point to a slightly higher *p*-character of the Sb–Se bonds compared to that of the Sb–S bonds (close to 270° for pure *p*-character). Therefore, the Sb lone pair is of slightly higher *s*-character for the selenide, which might give an additional explanation for the longer Sb⋯Cu distance (weaker interaction) as observed for compound **2**.

The reaction conditions employed for the synthesis of both **1** and **2** are almost identical, so that the external factors, such as solvent, dosage and mole ratio of the reactants, temperature, and reaction time, have a less effect onto crystal morphology. Therefore the different crystal shapes of **1** and **2** might be related to their internal factors. Although both crystals are isostructural, as mentioned above, crystals of $CuSbS_2$ is brick-like and that of $CuSbSe_2$ is plank-like. This difference in morphology should be related to the crystal face growth of $CuSbQ_2$. As can be seen from Fig. 2a, the bulk crystal has bedded vein, which correspond to the layered structure characterized by crystal analysis. The thickness of the crystals is controlled by the growth rate of the main crystal face that parallel to the (001) plane. The secondary Sb⋯Cu (3.417(2) Å) and Sb⋯S (3.107(2) Å) interactions between the

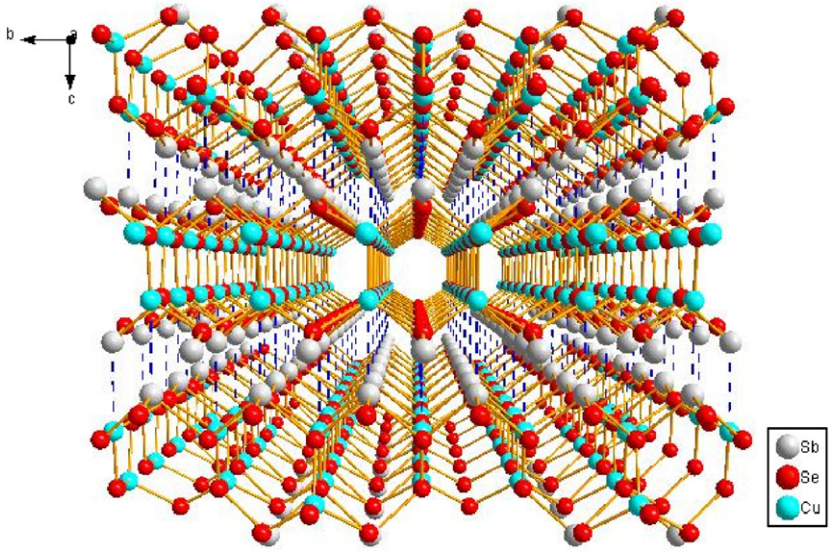

Fig. 4. 3-D extended network structure of **2**, in which the Sb···Cu interactions are connected and the Sb···S interactions are omitted for clarity.

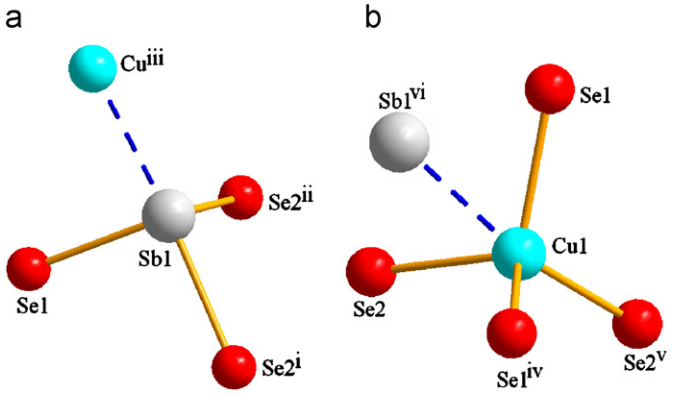

Fig. 5. Environment of Cu1 (a) and Sb1 (b) with labeling. Red dotted lines indicate long contacts. [Symmetry operation: (i) 1+*x*, *y*, *z*; (ii) 1+*x*, 1+*y*, *z*; (iii) *x*, 0.5+*y*, 1−*z*; (iv) *x*, −1+*y*, *z*; (v) 0.5+*x*, 1.5−*y*, 0.5−*z* ; (vi) −*x*, −0.5+*y*, 1−*z*].

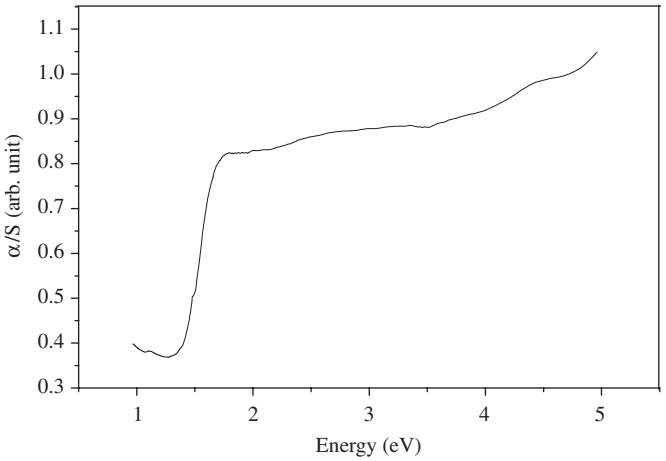

Fig. 6. Optical absorption spectrum of compound **1** derived from diffuse reflectance data.

adjacent $CuSbS_2$ layers are shorter than those in $CuSbSe_2$ (3.473(2) Å for Sb···Cu and 3.198(1) Å for Sb···Se). The short interaction distance and the close election density of *p* orbital for sulfur atom are attributes to the strong interactions between the main layers in $CuSbS_2$ crystal, which accelerate the crystal plane growth along the [001] direction (perpendicular to the main crystal face), resulting a thick $CuSbS_2$ crystal. The intensity of Sb···S > Sb···Se is also supported by the thermal data of *Q*–*X* bond energies [23].

3.3. Physical properties

The optical absorption properties of $CuSbQ_2$ are investigated with solid-state optical absorption spectroscopy (Fig. 6 and SI-Fig. 3). From the sharp absorption edges the band gaps can be estimated as 1.38 eV for **1** and 1.05 eV for **2**, suggesting that both samples are semiconductors with relatively small band gaps. The electronic absorptions are attributed to the lowest possible electronic excitation energy for charge-transfer processes in the $CuSbQ_2$. The optical band gap of **1** is slightly lower than that of $CuSbS_2$ thin films (1.52 eV) [1e]. This phenomenon could result from the different grain size of the materials (20 nm for thin film). The band

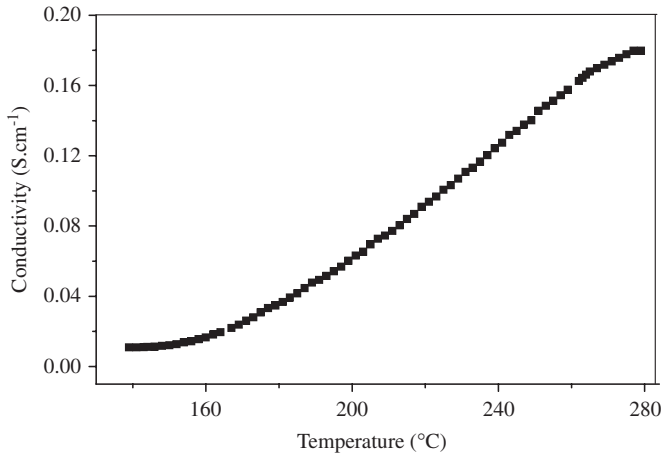

Fig. 7. Conductivities of compound **1** in variable temperature.

gap of **2** is lower than that of copper selenoantimonate containing organic components, such as, $Cu_2SbSe_3 \cdot 0.5en$ (1.58 eV) and $Cu_2SbSe_3 \cdot en$ (1.61 eV) [17]. To obtain further evidence for

semiconducting properties of both compounds, we have measured conductivity of them in variable temperatures (from 135 to 275 K). The electrical conductivities of $CuSbQ_2$ increase exponentially with increasing temperature, showing typical semiconducting behavior (Fig. 7 and SI-Fig. 4). The conductivity of **2** was somewhat higher than that of **1.** These experimental results are consistent with that the heavier chalcogenides displaying substantially higher electrical conductivity.

4. Conclusion

The purely inorganic copper-based chalcogenidoantimonates are generally obtained by high-temperature solid-state reaction, but relatively little is known about these crystals prepared by low-temperature solvothermal techniques, because organic structure-directing agents easily incorporate into the final structures. However, employing mild solvothermal method, we successfully isolate larger single crystals of $CuSbQ_2$. Their crystal structures were determined by single crystal X-ray diffraction. Both compounds have the double-layered arrangement, which is further interconnected by the secondary Cu⋯Sb and Sb⋯*Q* interactions to form a 3-D network structure. The stronger secondary interlayer interactions in $CuSbS_2$ accelerate the growth of (001) crystal face along the [001] direction, which results the thick brick-like crystals of $CuSbS_2$, compared with those plank-like crystals of $CuSbSe_2$. It should be a successful example to explain the macroscopical crystal growth by the microcosmic crystal properties.

Supplementary Information

Tables of selected bond lengths, angles and important secondary interactions, figures for XRD patterns, optical absorption spectrum and conductivity for **2** can be obtained from the Web. The CIF tables have been deposited with the Fachinformationszentrum Karlsruhe, D-76344 Eggenstein-Leopoldshafen (Germany). These data can be obtained free of charge *via* http://www.fiz-karlsruhe.de/icsd.html, or e-mail: crysdata@fiz-karlsruhe.de on quoting the depository number CSD # 418753 and 418754 for compounds **1** and **2**, respectively. See DOI:10.1039/b000000x/.

Acknowledgments

This work was supported by the National NSF (20371033), PR China, and by the NSF of the Education Committee of Guangxi Province. The authors are also grateful to Suzhou University, for financial support.

Appendix A. Supporting Information

Supplementary data associated with this article can be found in the online version at doi:10.1016/j.jssc.2008.10.025.

References

[1] A. Wachtel, A. Noreika, J. Electron. Mater. 9 (1980) 281–297;
G.B. Abdullaev, A.U. Mal'sagov, V.M. Glazov, Inorg. Mater. 4 (1968) 1082–1084;
I. Grigas, N.N. Mozgova, A. Orlyukas, V. Samulenis, Sov. Phys. Crystallogr. 20 (1976) 741–1742;
V.P. Zhuse, V.M. Sergeeva, E.L. Shtrum, Sov. Phys. Tech. Phys. 3 (1958) 1925–1938;
Y. Rodríguez-Lazcano, M.T.S. Nair, P.K. Nair, J. Cryst. Growth 223 (2001) 399–406.
[2] A.Z. Pfitzner, Anorg. Allg. Chem. 621 (1995) 685–688;
A.Z. Pfitzner, Kristallografiya 209 (1994) 685.
[3] H. Su, Y. Xie, S. Wan, B. Li, Y. Qian, Solid State Ionics 123 (1999) 319–324.
[4] C. An, Q. Liu, K. Tang, Q. Yang, X. Chen, J. Liu, Y. Qian, J. Cryst. Growth 256 (2003) 128–133.
[5] S. Manolache, A. Duta, L. Isac, M. Nanu, A. Goossens, J. Schoonman, Thin Solid Films 515 (2007) 5957–5960.
[6] W. Hofmann, Z. Kristallogr. Kristallgeom. Kristallphys. Kristallchem. 84 (1933) 177–178;
M.F. Razmara, C.M.B. Henderson, R.A.D. Pattrick, Min. Mag. 61 (1997) 79–88.
[7] A. Kyono, M. Kimata, Am. Min. 90 (2005) 162–165.
[8] R.M. Imamov, Z.G. Pinsker, A.I. Ivchenko, Kristallografiya 9 (1964) 853–856.
[9] D.J. Vaughan, J.R. Craig, Mineral Chemistry of Metal Sulfides, Cambridge University Press, Cambridge, 1978;
K. Tan, Y. Ko, J.B. Parise, A. Darovsky, Chem. Mater. 8 (1996) 448–453.
[10] W.W. Wendlandt, H.G. Hecht, Reflectance Spectroscopy, Interscience Publishers, New York, 1966.
[11] G.M. Sheldrick, SHELXS-97, Program for Crystal Structure Determination, University of Göttingen, Göttingen, Germany, 1997.
[12] G.M. Sheldrick, SHELXL-97, Program for the Refinement of Crystal Structures, University of Göttingen, Göttingen, Germany, 1997.
[13] A.V. Powell, R. Paniagua, P. Vaqueiro, A.M. Chippindale, Chem. Mater. 14 (2002) 1220–1224.
[14] V. Spetzler, H. Rijnberk, C. Näther, W. Bensch, Z. Anorg. Allg. Chem. 630 (2004) 142–148.
[15] V. Spetzler, C. Näther, W. Bensch, Inorg. Chem. 44 (2005) 5805–5812.
[16] A.V. Powell, S. Boissière, A.M. Chippindale, J. Chem. Soc. Dalton Trans. (2000) 4192–4195.
[17] Z. Chen, R.E. Dilks, R.-J. Wang, J.Y. Lu, J. Li, Chem. Mater. 10 (1998) 3184–3188.
[18] D.-X. Jia, J. Dai, Q.-Y. Zhu, Y. Zhang, X.-M. Gu, Polyhedron 23 (2004) 937–942;
J. Li, Z. Chen, R.-J. Wang, D.M. Proserpio, Coord. Chem. Rev. 190–192 (1999) 707–735.
[19] V. Spetzler, C. Näther, W. Bensch, J. Solid State Chem. 179 (2006) 3541–3549;
P. Vaqueiro, A.M. Chippindale, A.R. Cowley, A.V. Powell, Inorg. Chem. 42 (2003) 7846–7851.
[20] A.V. Powella, J. Thuna, A.M. Chippindale, J. Solid State Chem. 178 (2005) 3414–3419.
[21] S.-Z. Hu, Z.-H. Zhou, K.-R. Tsai, Acta Phys. Chim. Sin. 19 (2003) 1073–1077.
[22] H. Stephan, M.G. Kanatzidis, J. Am. Chem. Soc. 118 (1996) 12226–12227;
H. Stephan, M.G. Kanatzidis, Inorg. Chem. 36 (1997) 6050–6057;
W. Bensch, C. Näther, R. Stähler, Chem. Commun. (2001) 477–478;
D.X. Jia, Y. Zhang, Q. Zhao, J. Deng, Inorg. Chem. 45 (2006) 9812–9817.
[23] R.C. Weast (Ed.), Handbook of Chemistry & Physics, 70th Ed., 1989–90, CRC Press, F-197.